Progress of Theoretical Physics, Vol. 80, No. 3, September 1988

Vortices, Superfluidity and Phase Transition in ^{4}He Film Adsorbed on Porous Materials

Tomoki MINOGUCHI and Yosuke NAGAOKA

Department of Physics, Nagoya University, Nagoya 464

(Received April 9, 1988)

We investigate the superfluid transition of ^{4}He thin film adsorbed on porous materials with emphasis on the role of vortices. Considering the multi-connectivity of the film, we show that the interaction among the vortices excited in the film is essentially one dimensional due to the quantum behavior of the flow. As a result, it is generally shown that the vortices do not dissociate at T_λ where the long range order (LRO) vanishes in contrast to the two dimensional case.

We also study the mechanism of dissipation for applied AC flow with the frequency ω, noting that a finite dimension of the film, the pore size a, plays an important role. The crossover phenomena between the Kosterlitz-Thouless transition and the λ transition are predicted: The superfluid onset is accompanied with the disappearance of the free vortices in large a or high ω cases, whereas with the appearance of the LRO in small a or low ω cases.

Our theory qualitatively explains various experimental results with the torsion pendulum.

§ 1. Introduction

After a stimulating work of Berezinskii,[1] the famous Kosterlitz-Thouless (KT) theory was presented where the importance of the correlation of topological excitations was pointed out and a sharp transition was predicted in purely 2D systems.[2),3)] In the ^{4}He thin film it was shown that the superfluid density ρ_s suddenly vanishes at a finite temperature T_{KT} where vortex pairs dissociate. Such a prediction was against a conventional understanding that a sharp transition never exists in 2D systems because of large fluctuations. Many experiments began to confirm it.

In the first stage, because of the large surface area porous materials such as Vycor glass[4] were introduced as good adsorbents for the purpose of investigating whether the adsorbed ^{4}He thin film experiences the superfluid transition or not. Many interesting properties of the adsorbed film in porous materials were found out about the superfluid transition. However, such a system is not a simple 2D film but a multiply-connected one composing a 3D network as in Fig. 1. By those experiments, therefore, everybody was not convinced of the occurrence of the superfluid transition in the purely 2D system.

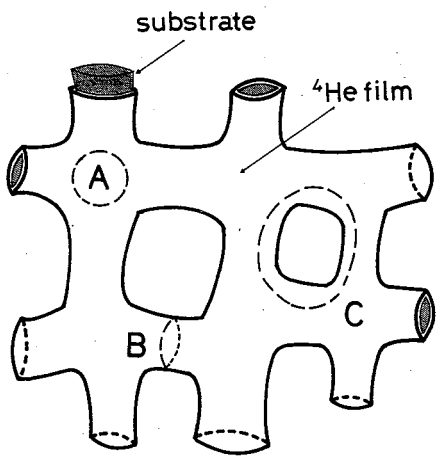

Fig. 1. ^{4}He film adsorbed on a porous material.

In 1978 Bishop and Reppy succeeded in observing the superfluid transition in a purely 2D system, a few atomic layer of

^{4}He on a Mylar sheet[5] by the torsion pendulum measurement. To compare the KT theory with this measurement, Ambegaokar et al. extended it to include the dynamical perturbation[6] within the linear response theory. In this dynamical theory, the real part of the response coefficient to the external oscillation corresponds to ρ_s and the imaginary one to the energy dissipation of the pendulum. A peak of the energy dissipation at T_{KT} was predicted in addition to the sharp drop of ρ_s due to the vortex pair dissociation. These predictions were completely realized in the experiment.

Now there remain interesting problems for the films on porous materials because they experience the superfluid transition in apparently different ways from the purely 2D case. Recently the experiments were extensively carried out mainly with the torsion pendulum technique[7)~9)] and with the third sound propagation method.[10] The common features in these experimental results are that the superfluid onset temperature T_0 is quite near to T_{KT} and that ρ_s continuously drops at T_0. There are, however, some differences in the critical behaviors of ρ_s as follows.

Reppy and his co-workers employed Vycor glass whose pore size is about 100 Å.[7),8)] They found that the critical exponent ζ defined by $\rho_s \propto |T - T_0|^{\zeta}$ is quite near to 2/3, the value in the pure bulk system. They concluded that the λ transition takes place in the Vycor glass because the global structure is 3D. The local structure, however, is 2D and then vortices will be excited in the film. They will play an important role in the superfluid transition with increasing pore size because the film tends to the purely 2D system. Then it is interesting, if their explanation is correct, to investigate why vortices are irrelevant to the transition in 100 Å Vycor case.

Kotsubo and Williams proposed the other explanation: the KT transition with finite size broadening takes place. They measured the third sound propagation in ^{4}He film on the packed fine powder of Al_2O_3 by varying the grain size: about 1 μm, 3000 Å and 500 Å. Because of the attenuation of the sound one cannot observe the behavior of ρ_s in the onset region. They found that the attenuation is lowered with decreasing grain size and in 500 Å case they confirmed that the drop of ρ_s is broadened.[10] Subsequently they calculated the stiffness of vortex-vortex interaction on a single sphere within the KT theory.[11] The drop of the stiffness between a couple of vortices on the opposite sides on the sphere, to be called the renormalized stiffness, becomes broader as the diameter of the sphere decreases because of the finite size effect. They pointed out that their experimental results are well explained by this sphere model whose diameter is taken to be the grain size, if the renormalized stiffness is identified with the observed quantity, ρ_s.

Shirahama et al. observed the superfluid transition of ^{4}He films on the three kinds of packed Pt fine powders whose grain sizes are respectively about 500 Å, 100 Å and 60 Å. They employed the same technique as Reppy and his co-workers did. Their results support the explanation of Kotsubo and Williams: They confirmed not only that the sharp transition, appeared in the 500 Å case, becomes broader as the grain size decreases, but that the energy dissipation peak appears at T_0 in all cases.[9] It suggests that the superfluid onset is accompanied with the disappearance of free vortices as is in the 2D case.

Some questions arise. First, why are the experimental results so different between those of Reppy and his co-workers and of Kotsubo and Williams and

Shirahama et al.? Three explanations will be possible:

i) The adsorbed film experiences the λ transition for small pore cases and the KT like one for large pore cases.

ii) The KT like transition takes place for any pore sizes. If so, the drop of ρ_s becomes broader with decreasing pore size and $\rho_s \propto |T - T_0|^{2/3}$ is accidentally observed for 100 Å case.

iii) The behavior of ρ_s is essentially different between on the Vycor glasses and on the pack fine powders.

Second, why is the single sphere model so successful for the experiments that Kotsubo and Williams and subsequently Shirahama et al. carried out? Especially,

a) why is vortex pair dissociation temperature estimated in such a model of only one grain, even though each film on the grains connect with each other to compose 3D network as in Fig. 1? and

b) why does the observed quantity, ρ_s, coincide with the renormalized stiffness in the vortex-vortex interaction on the scale of the grain?

In this paper we investigate the superfluid transition in the ^{4}He thin film adsorbed on porous materials, considering both the multi-connectivity and the three dimensionality of the film. We study the behavior of vortices assuming that they are excited in the film, and will show that the explanation i) is reasonable.

We calculate the temperature T_c where vortex pairs dissociate. In our previous paper[12] we showed that vortices are strongly coupled with each other as if they are *one dimensional* Coulomb charges. As a result, we will explain a): T_c is determined as the temperature at which the order of the phase appears on the short length scale, the pore size, *not* on the long length one in contrast to the purely 2D system, and then the vortex pair dissociation is not accompanied with the thermodynamic phase transition. We will conclude that the thermodynamic transition results from the long wavelength excitations as is in the pure bulk system. In this sense the thermodynamic transition temperature T_λ, where the long range order (LRO) appears, should be determined independently of T_c.

We study the mechanism of the dissipation of the applied flow with the frequency ω, because ρ_s is dynamically observed in the experiments. As a result, for sufficiently large pore cases or high ω cases we obtain essentially the same results as Kotsubo and Williams proposed: $T_0 = T_c$. We will give reasonable explanations to the question b). For small pore or low ω cases we will show that the λ transition should take place: $T_0 = T_\lambda$ as Reppy and his co-workers assert.

In the next section, we calculate the temperature T_c by using the KT theory. In § 2.1, a brief review of the KT theory is given. In § 2.2, we evaluate the interaction between vortices excited in the multiply-connected film. By considering explicitly the multi-connectivity of the film, we show that vortices interact one dimensionally with each other due to the quantum behavior of flows, which was briefly shown in Ref. 12). The calculation of T_c is given in § 2.3. We there emphasize that the KT theory is merely a mean field theory and then is inapplicable to the present case in the vicinity of T_c. T_λ is estimated in § 3. We investigate the dynamical properties in § 4 focusing the torsion pendulum experiment. There the crossover phenomena are predicted between the KT transition and the λ transition by varying the pore diameter a or the

frequency ω. We give a summary and discussion in § 5.

§ 2. Vortex pair dissociation in multiply-connected film

2.1. *Kosterlitz-Thouless theory in 2D systems*

Before discussing the multiply-connected film, we give a brief review of the KT renormalization theory in purely 2D system, which will be applied to the present problem in § 2.3. According to this theory the superfluid transition temperature T_{KT} and critical behaviors of the superfluid density ρ_s are determined by the correlation of excited vortices. As the reduction of ρ_s due to long wavelength excitations is sufficiently small compared with that due to vortices, one has only to take vortices into account to calculate ρ_s.

If $2N$ vortices are excited in the superfluid film, the Hamiltonian is given by

$$\mathcal{H}=-\frac{2}{\varepsilon_0}\sum_{i>j}\sigma_i\sigma_j \ln\frac{r_{ij}}{r_0}+2NE_c\,, \tag{2·1}$$

where r_{ij} is the distance between i-th and j-th vortices, σ_i the vorticity of the i-th vortex ($|\sigma_i|=1$), r_0 the diameter of vortex core and

$$\frac{1}{\varepsilon_0}\equiv\pi\kappa^2\rho_0\,,\quad \left(\kappa\equiv\frac{\hbar}{m}\right) \tag{2·2}$$

is a local stiffness with m and ρ_0 being the atomic mass and the local superfluid density respectively. E_c is the vortex core energy. As is well known, this system is equivalent to the 2D Coulomb gas with the dielectric constant ε_0 if vortices are regarded as charges.[13]

At sufficiently low temperatures $T\ll E_c$, a plus-vortex combines with a minus-one to compose a vortex pair. Then as the low temperature approximation of (2·1), we have the following Hamiltonian of vortex pairs:

$$\mathcal{H}\simeq\frac{2}{\varepsilon_0}\sum_{i=1}^{N}\ln\frac{r_i}{r_0}+2NE_c+\mathcal{H}_{p\text{-}p}\,, \tag{2·3}$$

where r_i is the length of the i-th pair and $\mathcal{H}_{p\text{-}p}$ is the interaction among the pairs. This system behaves as a dielectric medium. If a couple of test charges with opposite sign are located with separation r, the smaller pairs with $r_i\lesssim r$ are polarized and the larger pairs with $r_i\gtrsim r$ are not. So we can regard this system as a dielectric medium in a mean-field sense with the scale-dependent dielectric constant $\varepsilon(r)$ due to the polarization of pairs with $r_i\lesssim r$. We want to calculate $\varepsilon(\infty)$ which corresponds to ρ_s:

$$\frac{1}{\varepsilon(\infty)}=\pi\kappa^2\rho_s \tag{2·4}$$

in analogy with (2·2).

To calculate $\varepsilon(\infty)$ we shall apply the mean field approximation as follows. Instead of considering $\mathcal{H}_{p\text{-}p}$ explicitly, we treat non-interacting vortex pairs in which a plus-vortex interacts with a minus-one in the effective medium with $\varepsilon(r)$ to be

self-consistently determined. The Hamiltonian (2·3) is thus reduced to

$$\mathcal{H} \simeq 2\sum_{i=1}^{N}\int_{r_0}^{r_i} dr \frac{1}{r\varepsilon(r)} + 2NE_c \,. \tag{2·5}$$

The dielectric constant $\varepsilon(\infty)$ is given by

$$\varepsilon(\infty) = \varepsilon_0 + 4\pi\alpha \,, \tag{2·6}$$

where

$$\alpha \equiv \frac{1}{2} n\beta \langle r^2 \rangle \tag{2·6·1}$$

is the polarizability with

$$\langle r^2 \rangle = \frac{\int_{r_0}^{\infty} dr\ r^3 e^{-\beta E(r)}}{\int_{r_0}^{\infty} dr\ r e^{-\beta E(r)}} \,, \tag{2·6·2}$$

$$E(r) \equiv \int_{r_0}^{r} \frac{2dr}{r\varepsilon(r)} + 2E_c \,, \tag{2·6·3}$$

and n is the vortex pair density

$$n = \frac{1}{r_0^4}\int_{r_0}^{\infty} dr\ 2\pi r e^{-\beta E(r)} \,. \tag{2·6·4}$$

By substituting Eqs. (2·6·1)~(2·6·4) into Eq. (2·6), we have

$$\varepsilon(\infty) = \varepsilon_0 + 4\pi\int_{r_0}^{\infty} dr\ 2\pi r\ n(r)\frac{\beta}{2} r^2 \,, \tag{2·7}$$

where

$$n(r) = \frac{1}{r_0^4} e^{-\beta E(r)} \tag{2·8}$$

is the density of the pairs with the length r. Taking the derivatives of $\varepsilon(r)$ and $n(r)$ in Eqs. (2·7) and (2·8), we obtain the following recursion relations:

$$\varepsilon(r+dr) = \varepsilon(r) + 4\pi \cdot 2\pi r dr\ n(r)\frac{\beta}{2} r^2 \,,$$

$$n(r+dr) = n(r)\exp\left\{-\beta\frac{2dr}{r\varepsilon(r)}\right\} \,. \tag{2·9}$$

These are the well-known Kosterlitz recursion relations.[3),13)] With an initial condition

$$\varepsilon(r_0) = \varepsilon_0 \,,$$

$$n(r_0) = \frac{1}{r_0^4} e^{-2\beta E_c} \,, \tag{2·10}$$

we can obtain $\varepsilon(\infty)$ or ρ_s by iteration. The results are consistent with experiments

including a well-known drastic change of ρ_s at T_{KT}.[5]

2.2. *Vortex-vortex interaction in multiply-connected films*

Before discussing the correlation of vortices in the multiply-connected films, we should bear in mind some features of the superfluid flow occurring in the film. That is, the superfluid circulation along any closed path on the film should be quantized. For instance, the circulation along a dashed loop in Fig. 1 is quantized. The quantization in a simply connected region (like A in Fig. 1) leads to the quantized vorticity of vortices. The quantization around a channel (like B) leads to the non-trivial interaction among vortices as described later. It is also to be noted that the circulation is quantized along a closed path (like C) which cannot be shrunk to a point. The quantum number of the circulations along B and C are respectively result from the times of the passages of a vortex through the channel and the drifts around it.

Now we evaluate the interaction among vortices excited in the multiply-connected film. As remarked above, the quantization of the superfluid circulation around a channel is important. Let us suppose a couple of unit vortices excited in the film. If one is in the flow induced by the other, one is attracted or repelled by the Magnus force, resulting in the vortex-vortex interaction. We first show how a unit vortex induces superfluid current in the multiply-connected films, and next evaluate the vortex-vortex interaction.

For convenience, we introduce the XY-spin representation where the magnitude and the phase of the spin respectively represent those of the condensate wave function. If the fluid is assumed to be incompressible, the gradient of phases in the spin system represents the superfluid flow with velocity

$$\boldsymbol{v}_s=\kappa\boldsymbol{\nabla}\phi(\boldsymbol{r}), \tag{2·11}$$

where ϕ is a phase at a point $\boldsymbol{r}$.

In the purely 2D case such a spin configuration as in Fig. 2(a) represents a unit vortex. As the superfluid velocity $\boldsymbol{v}_s$ is represented by (2·11), the superfluid circulation occurs symmetrically around the center of vortex. If we impose a periodic boundary condition, however, we have unusual, asymmetric circulation. As shown in Fig. 2(b), directions of spins located on the upper boundary must coincide with those on the lower boundary. To make 2π gradient of the phase along a closed path surrounding the vortex core, only two kinds of configurations are possible such as to make the gradient along only half part of the path, right-hand side or left-hand side as in Fig. 2(b). Such a configuration represents the circulation induced only in the half side of the unit vortex. In other words, in the superfluid film on a cylinder the induced circulation by a unit vortex takes place asymmetrically because of the quantization of circulation around the cylinder. The unit vortex produces the unit circulation around the cylinder at large distances, which obviously cannot be divided into any fractional ones due to the quantum effect. This is the reason why the circulation takes place asymmetrically.

This leads to the following important fact: Even if the cylinder has branches, this circulation does not divide or spread out but goes into only one of branches keeping its magnitude unity as shown in Fig. 2(c). So, in general, if a unit vortex is

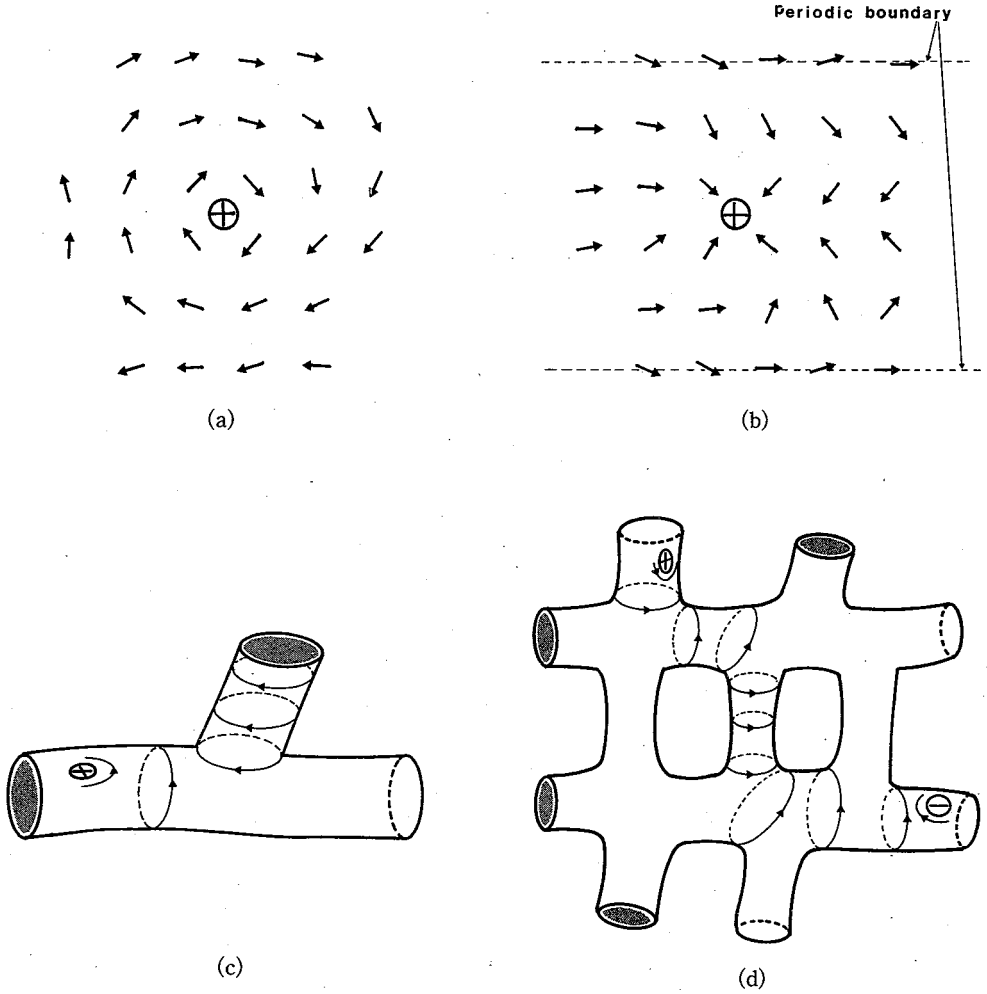

Fig. 2. (a) A unit vortex in a flat film.
(b) A unit vortex in a cylindrical film.
(c) Schematic description of the induced flow by a unit vortex on the branching cylinder. The quantization of circulation around one branch yields an image charge on the root coupling to the original vortex, which results in the charge-neutrality or the zero-circulation around the other.
(d) A string, which mediates the vortex-vortex interaction.

excited in the multiply-connected film with the pore diameter a, the velocity of the induced current reduces two dimensionally as $|v_s| \sim h/(mr)$ at $r \lesssim a$, where r is the distance from the vortex core, and remains constant $|v_s| \sim h/(ma)$ at $r \gg a$ in spite of the presence of many branches. Thus the vortex-vortex interaction is essentially one-dimensional at large distances $r \gg a$, whereas two-dimensional at small distances $r \ll a$. At low temperatures, then *charge confinement* takes place so as to form a vortex-antivortex pair with a *string* of circulation connecting the two. (See Fig. 2(d).) It is interesting that vortices in the present geometry behave similarly to quarks in high energy physics. We note that Machta and Guyer also investigated this multiply-connected system and found the charge confinement independently of us.[14]

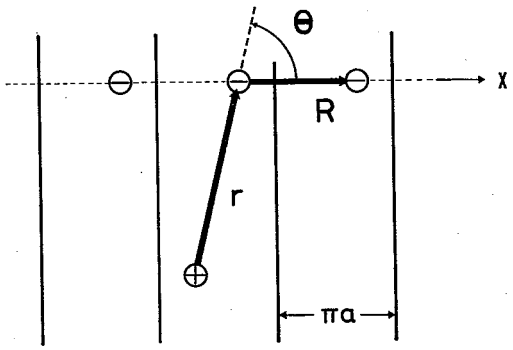

Fig. 3.

2.3. *Vortex pair dissociation*

In this subsection we calculate the temperature T_c where vortex pairs dissociate in the multiply-connected film. The reduction of the stiffness of the vortex-vortex interaction is assumed to be due to the interaction among pairs as in the 2D case. In the present system, as described at the end of the preceding subsection, the induced current due to a pair is bunched to make a string connecting a couple of vortices. So the interaction among pairs will be a very short range one. In other words pairs will hardly interact with each other except when one is in the string of the other. So the present system is essentially equivalent to the following model system so far as the vortex correlation is concerned: the ^{4}He film on a cylinder with diameter a and infinite length.

Within the KT renormalization theory, we calculate the stiffness or the dielectric constant and consequently T_c in the cylindrical model described above. We take the x-axis perpendicularly to the axis of cylinder as in Fig. 3. The interaction between a couple of unit vortices with opposite sign takes the following form:[12]

$$U_0(r,\theta)=\frac{2}{\varepsilon_0}\sum_{n=0,\pm1,\pm2\cdots}\ln\frac{|\boldsymbol{r}+n\boldsymbol{R}|}{\sqrt{r_0^2+n^2R^2}}, \tag{2·12}$$

where $\boldsymbol{r}$ is the vector separating a vortex pair and $\boldsymbol{R}\equiv\pi a\boldsymbol{i}$ with $\boldsymbol{i}$ being the unit vector of the x-axis. We put $r\equiv|\boldsymbol{r}|$, $R\equiv|\boldsymbol{R}|$ and $\theta\equiv\cos^{-1}(\boldsymbol{r}\cdot\boldsymbol{R}/(rR))$. At small distances $r\ll R$, we expand (2·12) with a small parameter r/R to obtain

$$U_0(r,\theta)\simeq\frac{2}{\varepsilon_0}\left\{\ln\frac{r}{r_0}-\frac{\pi^2}{6}\left(\frac{r}{R}\right)^2\cos2\theta\right\}. \tag{2·13}$$

At large distances $r\gg R$, on the other hand, we can replace the summation with the integration:

$$\sum_n\to\frac{r}{R}\int_{-\infty}^{\infty}d\left(n\frac{R}{r}\right) \tag{2·14}$$

and have

$$U_0(r,\theta)\simeq\frac{2\pi}{\varepsilon_0}\frac{r}{R}. \tag{2·15}$$

That is, the interaction is one dimensional at large distances and two dimensional at small distances.

Employing $U_0(r,\theta)$, we obtain the extended Kosterlitz recursion relations for the cylindrical system via the same procedure as in § 2.1:*)

*) Note that the dielectric constant $\varepsilon(r,\theta)$ and the vortex pair density $n(r,\theta)$ depend on two parameters r and θ because of the anisotrophy of the interaction $U_0(r,\theta)$.

$$\varepsilon(r+dr,\theta)=\varepsilon(r,\theta)+4\pi\int d\theta' r dr\, n(r,\theta')\cdot a(r,\theta,\theta'),$$

$$n(r+dr,\theta)=n(r,\theta)\cdot\exp\left\{-\beta\frac{\partial U(r,\theta)}{\partial r}dr\right\}, \tag{2·16}$$

where

$$a(r,\theta,\theta')=\beta r^2\cos^2(\theta-\theta') \tag{2·16·1}$$

and*)

$$\int\equiv\begin{cases}\displaystyle\int_0^{2\pi}, & (r<R/2)\\ \displaystyle\int_{\theta_c}^{\pi-\theta_c}+\int_{\pi+\theta_c}^{2\pi-\theta_c}, & (r>R/2)\end{cases} \tag{2·16·2}$$

with the cutoff angle

$$\theta_c\equiv\cos^{-1}\left(\frac{R}{2r}\right). \tag{2·16·3}$$

We put

$$U(r,\theta)=\int_{r_0}^{r}dr\frac{\varepsilon_0}{\varepsilon(r,\theta)}\frac{\partial U_0(r,\theta)}{\partial r}, \tag{2·16·4}$$

which is the renormalized potential of a vortex pair with the separation r and the angle θ. The initial condition is given by

$$\varepsilon(r_0,\theta)=\varepsilon_0,$$
$$n(r_0,\theta)=\exp(-2\beta E_c)/r_0^4. \tag{2·17}$$

Before calculating the renormalized dielectric constant $\varepsilon_R\equiv\varepsilon(\infty,\theta_c)$, we give a note connected with the inapplicability of the recursion relations to the 1D regime $r\gg R$. To see this, we first calculate ε_R for the 1D limit $R\to r_0$ in Eqs. (2·16). In the case $R\ll r$, the cutoff angle is

$$\theta_c\simeq\frac{\pi}{2}-\frac{R}{2r}, \tag{2·18}$$

which results in

$$\int\simeq\frac{R}{r}\int d\theta\left\{\delta\left(\theta-\frac{\pi}{2}\right)+\delta\left(\theta-\frac{3}{2}\pi\right)\right\}. \tag{2·19}$$

By substituting (2·19) and (2·15) into (2·16), we obtain the recursion relations for the 1D Coulomb gas as

$$\varepsilon_1(r+dr)=\varepsilon_1(r)+4\pi\cdot 2dr\, n_1(r)\beta r^2,$$

*) In Ref. 12) the definition of $\int$ should be replaced as in (2·16·2).

$$n_1(r+dr)=n_1(r)\exp\left\{-\beta\frac{2\pi}{\varepsilon_1(r)}dr\right\}, \tag{2·20}$$

where we set $R=r_0$ and put $\varepsilon_1\equiv r_0\varepsilon(r)$ and $n_1\equiv r_0^2 n(r)$. With the starting values

$$\varepsilon_1(r_0)=r_0\varepsilon_0,$$
$$n_1(r_0)=\exp(-2\beta E_c)/r_0^2, \tag{2·21}$$

it is resulted that $\varepsilon_R^{(mf)}$ (hereafter we use the superscript '(mf)' for ε_R calculated by the recursion relations) diverges at some finite temperature $\sim E_c$ (see the Appendix for the detail).

This result must be considered as an artificial one because it is inconsistent with the rigorous theory of Edwards and Lenard where the possibility of a thermodynamic phase transition is excluded in the 1D Coulomb gas.[15] This inconsistency comes from the inapplicability of the Kosterlitz recursion relations where, as was pointed out in § 2.1, the mean field approximation is employed.

In Ref. 15), the reduced density function $f_{\sigma,\sigma'}(r)$ is given for the two particles of charge σ and σ' with the separation r in Eq. (114). With this function, we can obtain

$$\varepsilon_R-\varepsilon_0\sim 4\pi\beta\int_{r_0}^{\infty}dr\ r^2 f_{1,-1}(r). \tag{2·22}$$

It is shown that $f_{1,-1}(r)$ is a monotone decreasing function of r, and that the system falls into the plasma state in the high temperature limit. As the thermodynamic phase transition is excluded, we then conclude that ε_R increases continuously as the temperature T increases and diverges only when $T\to\infty$, or that pairs never dissociate at finite temperatures.

As for the cylindrical case, and equivalently for the multiply-connected case, we obtain ε_R in a good approximation by replacing ε_0 in (2·22) with $\varepsilon(R/2, 0)$:

$$\varepsilon_R-\varepsilon\left(\frac{R}{2},0\right)\sim 4\pi\beta\int_{R/2}^{\infty}dr\ r^2\tilde{f}_{1,-1}(r), \tag{2·23}$$

where $\tilde{f}_{1,-1}(r)$ is given by replacing ε_0 in $f_{1,-1}(r)$ with $\varepsilon(R/2, 0)$, and $\varepsilon(R/2, 0)$ is obtained by the iteration up to the scale $r=R/2$ in the recursion formula (2·16). The right-hand side of (2·23) is due to the screening of pairs with $r\gg R/2$, which cannot be calculated by (2·16). From the results in the 1D case, we can conclude that ε_R diverges at the temperature T_c where $\varepsilon(R/2, 0)$ does and then T_c is given by

$$\frac{1}{\left[\varepsilon\left(\frac{R}{2},0\right)\right]_{T=T_c}}=0. \tag{2·24}$$

At $T=T_c$, $\varepsilon(r, 0)$ diverges at $r=R/2$, whereas remains finite at $r<R/2$. In other words, the interaction is present only when the separation between a couple of vortices is smaller than $R/2$. The mean distance of the free vortices at T_c is then $R/2$.

In the purely 2D case,[13] it is established that the mean distance of the free vortices is comparable to the phase correlation length ξ, which is given in $T\gtrsim T_{KT}$ by

$$\xi(T)\sim r_0\exp\left\{\frac{1}{b\sqrt{T-T_{KT}}}\right\}, \tag{2·25}$$

where b is a constant which depends on the details of the system. We believe that the periodic boundary condition has little effect on the correlation of vortices on the short length scales $r\lesssim R/2$ and that (2·25) still holds in the present problem. Then (2·24) is replaced by

$$\xi(T_c)\sim\frac{R}{2}. \tag{2·26}$$

The vortex pair dissociation is then not accompanied with the thermodynamic phase transition in general because thermodynamic singularities appear when ξ diverges. Such a situation is obviously different from the 2D case.

By substituting (2·25) into (2·26), we obtain

$$T_c\sim T_{KT}+\frac{1}{\left(b\ln\frac{R}{2r_0}\right)^2}. \tag{2·27}$$

This result coincides with that in the single sphere model,[16] although the interconnectivity of the film is taken into account. Near T_c we have shown that vortices compose large pairs with long strings. Below T_c, however, the density of pairs with $r\gg R/2$ becomes considerably small due to the one dimensionality of the interaction. Such a situation will underlie the single sphere model.

If we put

$$\rho_s=\frac{1}{\pi\kappa^2\varepsilon_R} \tag{2·28}$$

in analogy with the 2D case, we regard ρ_s as the local superfluid density on the scale of a, because ρ_s appears at T_c determined by (2·26). As will be seen later, in the dynamical measurement this ρ_s is observed at high frequencies, for instance as the

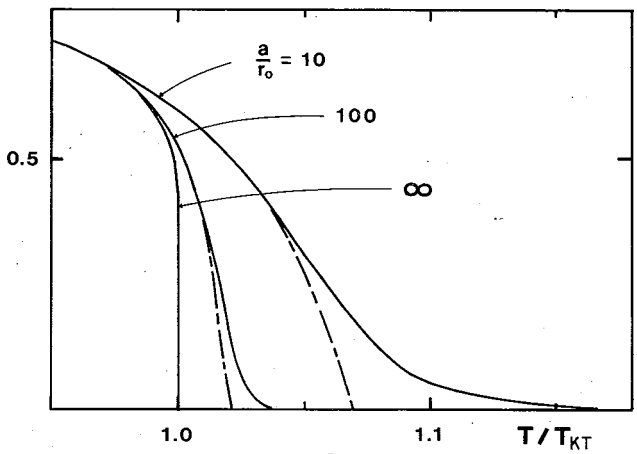

Fig. 4. $\varepsilon_0/\varepsilon_R$ or ρ_s/ρ_0 as a function of T. The solid and the dash-dotted lines respectively show $\varepsilon_0/\varepsilon(R/2,0)$ and $\varepsilon_0/\varepsilon_R^{(mf)}$. We set $E_c/(\kappa^2\rho_0)=2.2$.

period shift in the torsion measurement.

By employing (2·23), one can calculate ε_R in a good approximation. As $\tilde{f}_{1,-1}(r)$, however, is difficult to treat, here we represent ε_R by the following inequalities:

$$\varepsilon\left(\frac{R}{2}, 0\right) < \varepsilon_R < \varepsilon_R^{(mf)} . \tag{2·29}$$

At $T=T_c$, ε_R coincides with $\varepsilon(R/2, 0)$. We give in Fig. 4 both $\varepsilon(R/2, 0)$ and $\varepsilon_R^{(mf)}$ calculated by (2·16) with (2·17) as a function of T. When $a \gg r_0$, ρ_s suddenly vanishes at T_c, whereas continuously does when $a \gtrsim r_0$.

It is here noted again that ρ_s calculated above is merely a stiffness in the vortex-vortex interaction and that it does not necessarily coincide with that measured in the torsion or the third sound experiments. As will be seen in § 4, they coincide with each other only in the case of high frequency measurements or large a cases.

§ 3. Estimation of T_λ

In this section we estimate the thermodynamic transition temperature T_λ. We show that T_λ is determined independently of T_c where the vortex pair dissociation takes place. To confirm this, let us first consider the cylindrical ^{4}He film introduced in the preceding section. Using the XY spin representation, the spin-spin correlation function in the direction of the axis is given within the spin wave approximation by[17]

$$g(r) \equiv \langle \cos\phi(\mathbf{0}) \cos\phi(\boldsymbol{r}) \rangle \sim e^{-T/2\pi J(r/a + \ln r/r_0)} , \tag{3·1}$$

where $\boldsymbol{r}$ points along the direction of the axis, J is the coupling constant, a the diameter of the cylinder, and ϕ and r_0 are again the phase of the XY spin and the healing length respectively. From (3·1), it is readily seen that there is no ordering state at any temperatures, or that $T_\lambda=0$. On the other hand, we have already shown that T_c is finite as in (2·27). Then the vortex pair dissociation takes place independently of the disappearance of LRO (or quasi-LRO) in contrast to the 2D case.

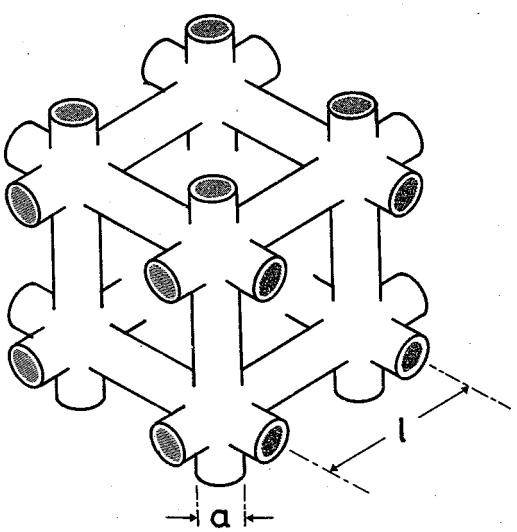

Fig. 5. Idealized geometry of the multiply-connected film.

Such a situation still holds in the 3D multiply-connected case. To make our problem clear, we shall consider such an idealized geometry as in Fig. 5 where the channel length l is much larger than the diameter a. With decreasing temperature, it is expected that three dimen-

sional properties appear when the phase correlation length $\xi \sim l$ and then the thermodynamic transition can take place.[18] When $\xi < l$, each cylindrical part composing the multiply-connected film may behave independently. Then the spin-spin correlation function may take the same form as (3·1). For large distances $r \gg a$, (3·1) reduces to

$$g(r) \sim e^{-Tr/2\pi Ja}, \tag{3·2}$$

which shows

$$\xi = \frac{2\pi Ja}{T}. \tag{3·3}$$

Then if we determine T_λ as

$$\xi(T_\lambda) \sim l, \tag{3·4}$$

we have

$$T_\lambda \sim 2\pi J \frac{a}{l}$$

$$\sim \frac{a}{l} T_{KT}. \qquad (l \gg a) \tag{3·5}$$

In such substrates as Vycor glass and packed fine powder, l is comparable to a. So as soon as ξ grows to a, where the vortex confinement takes place, ξ will diverge and the thermodynamic transition will appear. That is T_λ will be just below T_c.

§ 4. Phase slip mechanism and crossover phenomena

As is noted in § 2.3, the superfluid density ρ_s in the renormalized stiffness of the vortex-vortex interaction does not necessarily coincide with ρ_s observed in the experiments. We show in this section that ρ_s of the stiffness coincides with the observed value in the high frequency measurements, whereas it does not coincide with that in the low frequency ones.

In the experiments with the torsion pendulum we note that ρ_s is observed as a finite quantity unless the superfluid flow, which is driven by the mechanical oscillation, is completely dissipated during a period. Then we investigate how the flow is dissipated in such a multiply-connected film as in Fig. 5 by applying the Iordanskii-Langer-Fisher (ILF) theory[19),20] to the present problem.

In experiments substrates such as $l \sim a \sim 100$ Å are employed. By taking ω and A respectively as the frequency and the typical amplitude of oscillation, the driven flow has the velocity

$$v_s \sim A\omega \ll \frac{h}{ma}, \tag{4·1}$$

where we put $A \sim 10^{-10}$m and $\omega \sim 1$KHz. (4·1) means that the flow is driven only towards the axis of each channel and no flow around channels. Therefore we have only to investigate the dissipation mechanism for the axis flow with the velocity (4·1).

In usual systems ILF proposed the mechanism of the phase slippage due to vortices in the vicinity of the phase transition. In purely 2D film, for instance, ILF theory gives a critical size of vortex pair as[21]

$$r_c=\frac{h}{mv_s}, \tag{4·2}$$

where the free energy takes the maximum value $\Delta F(T, r_c)$. That is, if the pair with size $r>r_c$ is thermally activated, the driven flow is dissipated by expansion of the pair as $r\to\infty$. Smaller pairs with $r<r_c$ shrink and disappear, which yields no dissipation of the flow.

Before discussing the multiply-connected film, we first study the film on a long cylinder with diameter a again. On the cylinder the axis flow is dissipated by the activation of vortex pairs so as to expand along a circumference of the cross section of the cylinder and to shrink to a point on the other side. In the case of small velocity (4·1), r_c is larger than a and then a plays the same role as r_c: The free energy takes its maximum when two vortices locate on the opposite sides of the cylinder. In this case, ΔF becomes a function of a instead of r_c and is given by

$$\Delta F(T, a)=U\left(\frac{\pi a}{2}, 0\right), \tag{4·3}$$

where $U(r, \theta)$ is the renormalized potential of a vortex pair given in (2·16·4). The time for the activation is given by

$$\tau=\tau_0 e^{\beta\Delta F(T,a)}, \tag{4·4}$$

where τ_0^{-1} is the attempt frequency.[21]

If $\omega\tau\gg 1$, such an activation cannot take place in a period, which results in $\rho_s>0$. Such a superfluid density is to be called "apparent" one because there is no LRO in the cylindrical film as described in § 3. In this case superfluidity is observed unless the free vortices exist. In other words, the apparent superfluid density appears at T_c where the vortex confinement occurs. Thus we regard this apparent superfluid density as ρ_s of the stiffness given in (2·28) at least at T_c.

If $\omega\tau\ll 1$, typically for the DC flow, phase slippage by the vortex pair activation can occur during a period. It results in $\rho_s=0$ in the measurement, which is consistent with the fact that there is no LRO on the cylinder.

The multiply-connected film, such as in Fig. 5, is constructed by connecting the cylindrical films so as to compose a three dimensional network. Hereafter we shall consider the case $l\gg a$. Suppose the homogeneous DC flow driven with the small velocity $v_s\ll h/(ml)$. When $T>T_\lambda$, each cylinder composing the multiply-connected network may be regarded as independent. Then the phase slippage will take place via the same mechanism as in a cylinder. Therefore $\rho_s=0$ is measured in the DC flow measurement.

When $T<T_\lambda$, on the other hand, LRO appears and the phases at the junctions effectively couple with each other with the coupling energy, $\tilde{J}$. Then the phase slippage does not take place in the same way as in the simple cylindrical case. In this case superfluidity undergoes a qualitative change: Phase slippage no more takes

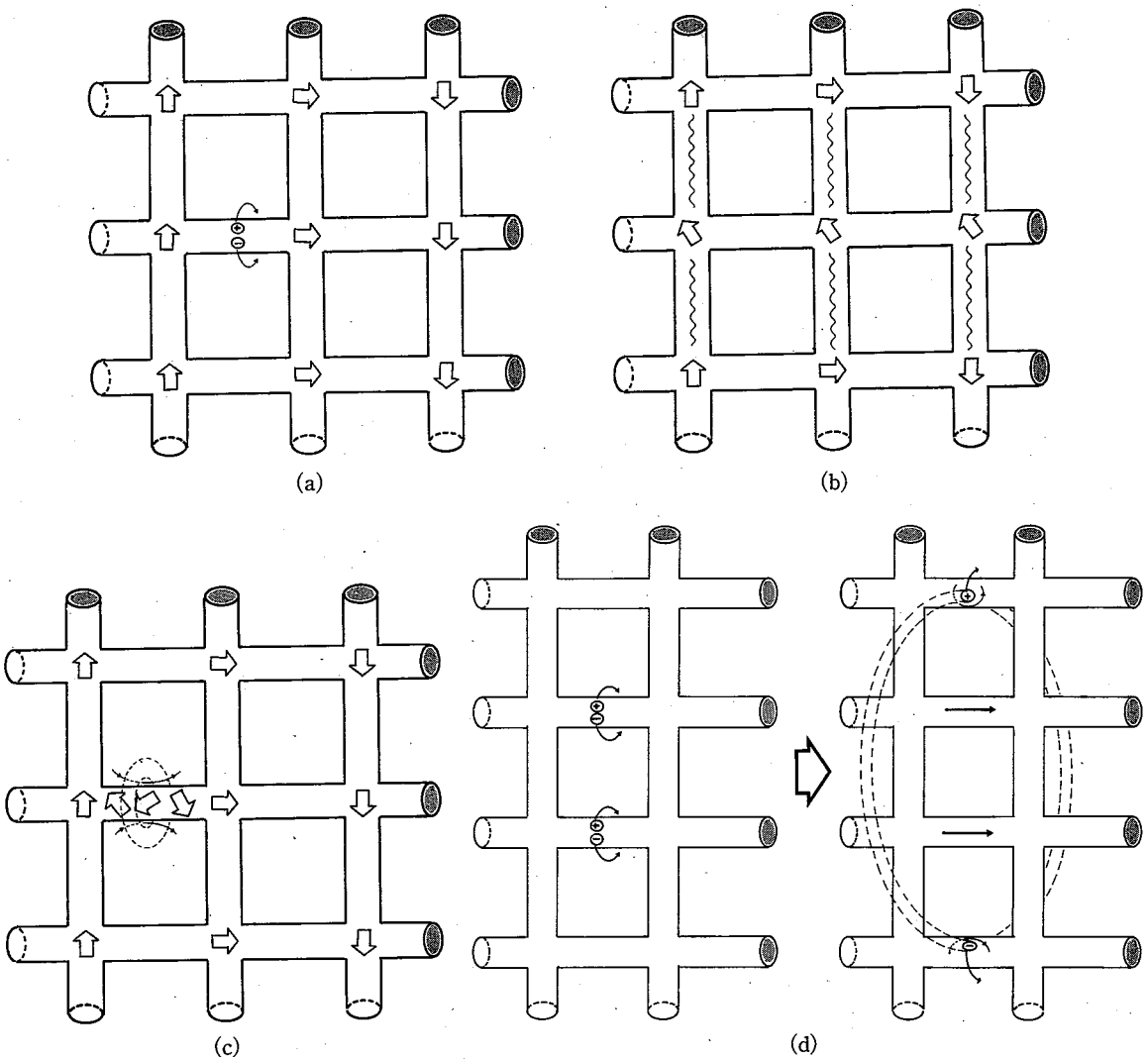

Fig. 6. The phase slip mechanism in the presence of LRO. The spins $\bar{S}(\boldsymbol{r})$ are illustrated by the white arrow marks. For simplicity, the spins between the junctions are omitted except when they are especially needed.
(a) The spin configuration representing the uniform flow applied from right to left. A vortex pair is thermally activated.
(b) Wave lines illustrate the misfits between the spins on the junctions. See the text for the detail.
(c) The favorable configuration resulting from the activation in (a). The local kink represents a back flow inside an imaginative "vortex ring" drawn by dashed curves.
(d) A large vortex ring can be created by the cooperative activation of the pairs. When the ring crosses the adsorbed film the cross sections correspond to the vortex pairs. The back flow, denoted by the bold arrow marks, is generated so as to reduce the applied flow.

place by the vortex pair activation as follows.

For convenience, we here again introduce the XY spin representation. Taking a spatial average over a local region $a\times a$ around a point $\boldsymbol{r}$, we have the averaged spin $\bar{S}(\boldsymbol{r})$. When $\xi\gg a$, since all phases in the region $a\times a$ are arranged to the same direction, we may consider only the phase of $\bar{S}(\boldsymbol{r})$ neglecting fluctuation of the

magnitude. In Fig. 6, we show various dynamical behaviors of $\bar{S}(\boldsymbol{r})$ in the presence of applied flow.

Suppose the uniform flow again, which is represented by such a spin configuration as in Fig. 6(a). When a vortex pair is thermally activated as shown there, the phase slippage no more takes place in the direction of the axis of the cylinder in contrast to the case $T > T_\lambda$. Because if it does, it generates the misfits among the spins on the junctions as shown in Fig. 6(b) which costs the excess energy $\sim \tilde{J}L/l$, which diverges as the system size L increases.

Such a configuration as in Fig. 6(c) is more favorable where the kink generated by the activation is not released but confined around the place where the activation has taken place. Such excitations are quite analogous to those in the bulk superfluid ^{4}He: This local kink corresponds to a small "vortex ring", to be dissipated in a short time via the inverse process of the activation.

Then if the applied flow is dissipated, we assert that it is due to the bulk-like phase slip mechanism. That is, the phase slippage is possible only when some vortex pairs are cooperatively activated to form the sufficiently large ring, as shown in Fig. 6(d). The time for the phase slippage in this case is then enhanced as

$$\tilde{\tau} = \tau e^{\beta \Delta \tilde{F}} \gg \tau , \tag{4·5}$$

where $\Delta\tilde{F}$ is a macroscopic free energy barrier to be determined in the three dimensional ordering. Here τ^{-1} given by Eq. (4·4) plays a role as the new attempt frequency in this system. So the DC flow is stable, as is in the true bulk system, and then $\rho_s > 0$ will be measured in DC flow measurements when $T < T_\lambda$. In AC flow measurements also, ρ_s will behave as in the true bulk system when $T < T_\lambda$.

When $v_s \gg h/(ml)$, there is a kink more than 2π in the spin configuration between the junctions of the film. One vortex pair activation generates a phase slip by 2π. Therefore the axis flow will be strongly dissipated to become $v_s \sim h/(ml)$ via the vortex pair activation even though LRO exists because such a phase slippage is possible with spins on the junctions being fixed, which yields no misfits among the spins. That is, the critical velocity in the multiply-connected system will be given by

$$v_{sc} \sim \frac{h}{ml} \tag{4·6}$$

in $T < T_\lambda$.

In essence, we assert that the 3D superfluid density is measured at any frequencies when $T < T_\lambda$, whereas the apparent one or the stiffness of the vortex-vortex interaction is also observed in high-frequency AC flow measurements when $T_\lambda < T < T_c$. This apparent superfluidity tends to disappear around $\omega\tau \sim 1$, where the superfluid onset temperature changes from T_c into T_λ. In this sense a crossover from the KT transition to the λ transition will take place with decreasing a or ω. We note that our results in the high ω case explain the experiments. For instance, the qualitative behaviors of ρ_s, rounding or drastic change in the vicinity of the onset temperature are consistent with the apparent superfluid density or the stiffness of the interaction

shown in Fig. 4.

§ 5. Summary and discussion

In this paper we have theoretically investigated the superfluid transition of the ^{4}He film adsorbed on porous materials considering both the three dimensionality and the multi-connectivity of the film.

We have calculated the temperature T_c where the vortex pair dissociation takes place in the film. Considering the multi-connectivity, we have shown that the vortex-vortex interaction is essentially one dimensional or that *vortex confinement* takes place because of the quantization of circulation occurring in the film. As a result, T_c is given by (2·26) or (2·27), where $a=R/\pi$ is the pore diameter of a substrate. We note that T_c is independent of the dimensionality of the connectivity.

If the connectivity is 3D, the thermodynamic phase transition temperature T_λ exists below T_c, where the phase correlation length ξ diverges. In other words, vortex pairs do not dissociate when LRO vanishes in contrast to the 2D case. If the channel length l is sufficiently large compared with the diameter a, as in Fig. 5, we obtain $T_c \gg T_\lambda$.

We have investigated the dissipation mechanism of the superfluid flow occurring in the present multiply-connected film. We note that the measured ρ_s in the torsion experiments does not necessarily coincide with ρ_s determined in the stiffness of the vortex-vortex interaction. We have predicted the crossover phenomena between the KT transition and the λ transition as follows. Because of the finite dimension of the film, the pore size a, vortex pairs can activate along the circumference of the cross section of the pore, which results in the dissipation of the applied flow. Through this process vortex pairs play the same role as free vortices as to the dissipation of flows. So the superfluid onset in the present system is not accompanied with the vortex binding, but the appearance of LRO, for the long time (low ω) observations.

For the short time (high ω) observations, however, the vortex pair activation does not take place during the period and then the superfluidity is observed unless free vortices appear. ρ_s in $T_\lambda < T < T_c$ experiences the universal jump as in 2D case for the large a limit, whereas continuously drops for small a cases as in Fig. 4.

In other words, there is a crossover frequency ω_c of the pendulum:

$$\omega_c \tau \sim 1 , \tag{5·1}$$

where τ is a characteristic time for the vortex pair activation and is a monotone increasing function of a given in (4·4) with (4·3). That is, the superfluid onset temperature T_0 coincides with T_c if $\omega\tau \gg 1$, whereas with T_λ if $\omega\tau \ll 1$.

In recent measurements employing the torsion pendulum, various kinds of critical behaviors of ρ_s have been observed. In the experiments by Berthold et al.[7] and subsequently by Crooker et al.,[8] the overall curves of ρ_s are 3D like and $\rho_s \propto |T - T_0|^{2/3}$ in the critical region except for small rounding at the onset. We note that such behaviors are consistent with our theory if the rounding behavior is identified with ρ_s of the stiffness to be observed in $T_\lambda < T < T_c$ and to disappear with decreasing

frequency of pendulum, ω.

The energy dissipation will be also predicted at T_c in our theory. In $T \lesssim T_c$, various sizes of vortex pairs are excited. Machta and Guyer pointed out[14] that long pairs with sizes $r \gg a$ do not contribute to the energy dissipation as follows. The free energy barrier in activation becomes smaller with increasing r and they respond as if they are free vortices for the axis flow. As free vortices hardly contribute to the energy dissipation,[6] it should be concluded that one has only to take small pairs $r \lesssim a$ into account to estimate the dissipation. It will yield essentially the same result as Wang and Yu[20] derived in the single sphere model,[11] where the weak dissipation, about 1/10 in magnitude compared with 2D case, is predicted.

In the experiment by Shirahama et al.,[9] this weak dissipation is found out at T_0, which suggests that the onset takes place at T_c. So what they measured, T-linear like behavior of ρ_s, is to be ρ_s of the stiffness. In fact their results quite resemble ρ_s shown in Fig. 4 and the quantities and the qualitative behaviors of T_0 are consistent with those of T_c given in (2·27).

In essence, the various experimental results that

i) $T_0 \sim T_{KT}$,

ii) T_0 slightly increases with decreasing a,

iii) there appears the energy dissipation peak at T_0,

iv) ρ_s experiences the finite jump at T_0 in large a cases, whereas continuously disappears in small a cases,

v) the overall curve of ρ_s is three dimensional,

can be explained in our theory of the case $\omega\tau \gg 1$.

Unfortunately, in the current substrates such as Vycor glass and packed fine powder l is comparable to a. It results in $T_\lambda \lesssim T_c$ and then T_0 may hardly be distinguished from the temperature where a peak of specific heat appears. Systematic torsion measurements with varying a or ω are especially interesting and desired.

After the completion of our work we received another preprint from Machta, where the thermodynamic phase transition is studied on the same line.[23]

Acknowledgements

We would like to thank K. Shirahama and N. Wada for valuable discussions on the experimental aspect and Y. Takano for sending the experimental data of Refs. 7) and 8). We are indebted to K. Miyake for useful comments on the phase slippage due to the activation of vortex pairs. We would also like to thank J. Machta and R. A. Guyer for sending preprints prior to publication.

Appendix

We here show that the recursion relations (2·20) for the 1D Coulombic system lead to a fictitious criticality. Introducing the dimensionless parameters

$$x \equiv \left\{\beta \frac{2\pi r}{\varepsilon_1(r)}\right\}^{-1} - \frac{1}{2}, \tag{A·1}$$

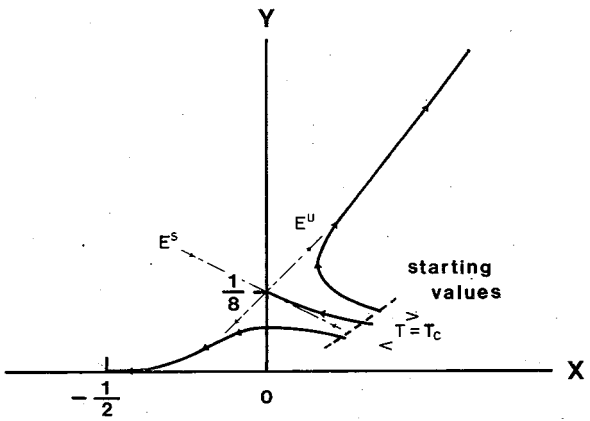

Fig. 7. Flow diagram for the recursion relations (A·4) and (A·5). E^s: $y=-1/4x+1/8$ and E^u: $y=1/2x+1/8$ are respectively the local stable and unstable eigenspaces.

$$y\equiv r^2 n_1(r) \tag{A·2}$$

and

$$l\equiv\ln\frac{r}{r_0}, \tag{A·3}$$

we have from (2·20)

$$\frac{dx}{dl}=4y-x-\frac{1}{2}, \tag{A·4}$$

$$\frac{dy}{dl}=2\left(1-\frac{1}{2x+1}\right)y. \tag{A·5}$$

With the starting values (2·21) or

$$x(l=0)=\left\{\beta\frac{2\pi r_0}{\varepsilon_1(r_0)}\right\}^{-1}-\frac{1}{2}, \tag{A·6}$$

$$y(l=0)=r_0^2 n_1(r_0)=e^{-2\beta E_c}, \tag{A·7}$$

there are a couple of fixed points where the right-hand sides of (A·4) and (A·5) are simultaneously zero. One is the sink point $(x, y)=(-1/2, 0)$ and the other is the saddle one $(0, 1/8)$. As shown in Fig. 7, all lines fall into the sink point if the temperature is sufficiently low compared with E_c or $2\pi r_0/\varepsilon_1(r_0)$. There we find

$$\frac{\varepsilon_1(L)}{\beta L}\to 0, \tag{A·8}$$

$$L^2 n_1(L)\to 0 \tag{A·9}$$

as the system size L increases. (A·8) means that $\varepsilon_1(L)$ does not diverge, or diverges more slowly than L. The latter, however, is to be excluded because (A·9) guarantees the lack of the long pairs or the free charges. Then the sink point corresponds to the insulating state.

At sufficiently high temperatures, every flow line diverges: $x, y\to\infty$ with $y/x=3/4$. That is,

$$\frac{\varepsilon_1(L)}{\beta L}\to\infty, \tag{A·10}$$

$$L^2 n_1(L)\to\infty. \tag{A·11}$$

(A·10) means that $\varepsilon_1(L)$ surely diverges, or that the system falls into the metallic state.

Then the saddle point corresponds to the criticality, the existence of which is inconsistent with the rigorous theory.[15] At the point, we find

$$\beta_c\frac{2\pi}{[\varepsilon_1(L)]_{T=T_c}}=\frac{2}{L}\to 0, \tag{A·12}$$

$$n_1(L)=\frac{1}{8L^2}\to 0\,, \qquad (A\cdot 13)$$

where T_c is the (fictitious) critical temperature. We verify that T_c is the order of E_c via numerical computation. (A·12) means that the continuous transition takes place, that is $1/\varepsilon_1(L)$ disappears continuously around T_c. This fictitious criticality generates the T-linear like critical behaviors of $\varepsilon_0/\varepsilon_R{}^{(mf)}$ in Fig. 4.

References

1) V. L. Berezinskii, Sov. Phys.-JETP **32** (1971), 493; **34** (1972), 610.
2) J. M. Kosterlitz and D. J. Thouless, J. of Phys. **C6** (1973), 1181.
3) J. M. Kosterlitz, J. of Phys. **C7** (1974), 1046.
4) M. H. W. Chan, A. W. Yanof and J. D. Reppy, Phys. Rev. Lett. **32** (1974), 1347.
5) D. J. Bishop and J. D. Reppy, Phys. Rev. Lett. **40** (1978), 1727; Phys. Rev. **B22** (1980), 5171.
6) V. Ambegaokar, B. I. Halperin, D. R. Nelson and E. D. Siggia, Phys. Rev. Lett. **40** (1978), 783; Phys. Rev. **B21** (1980), 1806.
7) J. E. Berthold, D. J. Bishop and J. D. Reppy, Phys. Rev. Lett. **39** (1977), 348.
8) C. Crooker, B. Hebral, E. N. Smith, Y. Takano and J. D. Reppy, Phys. Rev. Lett. **51** (1983), 666.
9) K. Shirahama, N. Wada, Y. Takano, T. Ito and T. Watanabe, Jpn. J. Appl. Phys. **26** (1987), Suppl. 26-3, 293 (*Proceedings of the 18th International Conference on Low Temperature Physics LT-18*).
10) V. Kotsubo and G. A. Williams, Phys. Rev. **B28** (1983), 440; **B33** (1986), 6106.
11) V. Kotsubo and G. A. Williams, Phys. Rev. Lett. **53** (1984), 691.
12) T. Minoguchi and Y. Nagaoka, Jpn. J. Appl. Phys. **26** (1987), Suppl. 26-3, 327 (*Proceedings of the 18th International Conference on Low Temperature Physics LT-18*).
13) B. I. Halperin, in *Physics of Low-Dimensional Systems,* ed. Y. Nagaoka and S. Hikami (*Proceedings of the Kyoto Summer Institute, 1979*).
14) J. Machta and R. A. Guyer, "Superfluid Films in Porous Media", Univ. of Massachusetts (August 11, 1987), Preprint.
15) S. Edwards and A. Lenard, J. Math. Phys. **3** (1962), 778.
16) G. A. Williams, Jpn. J. Appl. Phys. **26** (1987), Suppl. 26-3, 305 (*Proceedings of the 18th International Conference on Low Temperature Physics LT-18*).
17) D. J. Thouless, quoted in the article: P. Nightingale and H. Blöte, J. of Phys. **A16** (1983), L657.
18) See also T. Minoguchi and Y. Nagaoka, Prog. Theor. Phys. **78** (1987), 552.
19) S. V. Iordanskii, Sov. Phys.-JETP **21** (1965), 467.
20) J. S. Langer and M. E. Fisher, Phys. Rev. Lett. **19** (1967), 560.
21) J. S. Langer and J. D. Reppy, in *Progress in Low Temperature Physics,* ed. C. J. Gorter (North-Holland, Amsterdam, 1970), vol. VI, Chap. I.
22) C. Wang and L. Yu, Phys. Rev. Lett. **33** (1967), 599.
23) J. Machta and R. A. Guyer, Phys. Rev. Lett. **60** (1988), 2054.